Journal of Cell Science 112, 3283-3288 (1999)
Printed in Great Britain © The Company of Biologists Limited 1999
JCS0434

Microtubule bending and breaking in living fibroblast cells

David J. Odde[1,*], Le Ma[2], Amelie H. Briggs[1], Alyssa DeMarco[1] and Marc W. Kirschner[2]

[1]Department of Chemical Engineering, Michigan Technological University, Houghton, MI 49931, USA
[2]Department of Cell Biology, Harvard Medical School, Boston, MA 02115, USA
*Author for correspondence at present address: Department of Biomedical Engineering, University of Minnesota, Minneapolis, MN 55455, USA

Accepted 19 July; published on WWW 22 September 1999

SUMMARY

Microtubules in living cells frequently bend and occasionally break, suggesting that relatively strong forces act on them. Bending implies an increase in microtubule lattice energy, which could in turn affect the kinetics and thermodynamics of microtubule-associated processes such as breaking. Here we show that the rate of microtubule breaking in fibroblast cells increases ~40-fold as the elastic energy stored in curved microtubules increases to >~1 kT/tubulin dimer. In addition, the length-normalized breaking rate is sufficiently large (2.3 breaks·mm^{-1}·minute^{-1}) to infer that breaking is likely a major mechanism by which noncentrosomal microtubules are generated. Together the results suggest a physiologically important, microtubule-based mechanism for mechanochemical information processing in the cell.

Key words: Fluorescence microscopy, Cytoskeleton, Mechanochemistry, Tubulin, Molecular biomechanics

INTRODUCTION

Microtubules are linear filaments of the cytoskeleton that mediate such cellular processes as nerve growth and cell division and in general serve to organize the cytoplasm. In interphase cells microtubules tend to exhibit a radial pattern with the plus ends of microtubules pointing outward toward the cell periphery and the minus ends pointing inward toward the centrosome, near the nucleus. Distorting this archetypal pattern is the deformation of microtubules by cortical actin/myosin (Canman and Bement, 1997; Letourneau et al., 1987; Waterman-Storer and Salmon, 1997), manifested by varying degrees of microtubule curvature (Sammak and Borisy, 1988; Schulze and Kirschner, 1988; Tanaka et al., 1995). The presence of curvature indicates that the relatively stiff microtubules (Young's modulus ~10^9 Pa; Gittes et al., 1993) have elastic strain energy stored in them. The elastic strain energy increase in the microtubule lattice could in turn alter the kinetics and thermodynamics of processes associated with microtubules and provide a basis for mechanochemical signal transduction.

A variety of experimental results suggest that microtubules play a role in transducing mechanical stress into chemical responses. First, increasing tension on neurons promotes the assembly of microtubules (Zheng et al., 1993), consistent with thermodynamic models where reducing axial compression on microtubules promotes microtubule assembly over disassembly (Buxbaum and Heidemann, 1992; Hill, 1981). Similarly, stretching a monolayer of smooth muscle cells adherent to an equi-biaxially strained polymer substratum results in a net increase in microtubule assembly (Putnam et al., 1998). Second, analysis of *Caenorhabditis elegans* mutants implicates mec-7, a β-tubulin gene whose product forms an unusual 15 protofilament microtubule, as an essential component of the gentle-touch mechanosensory mechanism (Savage et al., 1989). Third, the sequence-specific transcription factor NF-κB, which mediates the fluid shear stress response in vascular endothelial cells (Khachigian et al., 1995), is activated by microtubule disassembly (Rosette and Karin, 1995). Together these results suggest that the chemical kinetics and thermodynamics of processes associated with microtubules are altered in response to mechanical deformation. However, there has not been any quantitative analysis of in vivo microtubule curvature, the associated elastic strain energies, and the impact of curvature on cellular processes.

One microtubule-associated process that is likely affected by mechanical deformation is microtubule breaking. Waterman-Storer and Salmon (1997) previously reported that a limited number of microtubule breaking events observed in rhodamine-tubulin injected newt lung cells occurred in microtubules with relatively high local curvature (average curvature = 1.7 rad/μm, n=7). However, the limited number of observations and lack of background curvature measurements (for microtubules that did not break) prevented the conclusive establishment of a relationship between bending and breaking.

To quantitatively determine the degree of microtubule curvature in living cells and the quantitative relationship between microtubule bending and breaking we analyzed individual microtubules at the leading edge of rhodamine-tubulin injected Swiss 3T3 fibroblasts. We found that the kinetics of microtubule breaking were accelerated when microtubules were curved to energy levels >1 kT/tubulin dimer. We also found that the amount of energy stored in the lattice as curvature-associated strain energy was ~2.5% of that associated with GTP hydrolysis, which occurs concomitantly

with assembly. In addition, we measured the breaking rate (on a per microtubule length basis) and, based on comparison to data in the literature, concluded that breaking is likely to be physiologically significant in terms of noncentrosomal microtubule generation in fibroblasts.

MATERIALS AND METHODS

Cell culture and videomicroscopy

Swiss 3T3 fibroblast cells were cultured overnight at 37°C in DMEM supplemented with 10% calf serum. Interphase cells were then injected with tetramethylrhodamine-labelled tubulin and cultured for 20 minutes. Fluorescent images were collected in the lamellum with a Zeiss Axiovert 135 microscope using a 63×, 1.4 NA objective and a cooled CCD camera under the control of Metamorph software running on a PC. Observation in this region of the cell facilitated the observation of single microtubules in a single focal focal plane. Digital images were collected every 3-10 seconds using a 0.1 second fluorescent illumination by a 100 W Hg arc lamp (note: the total illumination was <20% of that used by Vorobjev et al. (1997) and <50% of that used by Vigers et al. (1988) and photobleaching was negligible). The duration of experiments and number of breaking events in each sequence is summarized in Table 1.

Digital image analysis

Curvature was measured by selecting microtubules that could be clearly identified as individual filaments. Using Scion Image software running on a PC, the x-y coordinates of individual microtubules were recorded at approximately 0.5 μm intervals along their length. Curvature was then calculated at each point (excluding the two endpoints) by using the two adjacent points to calculate both the angle change ($\Delta\theta$) from one pair of points to the next and the contour length change (Δs, an average of the distances to the two neighboring points). Breaking events were recorded when a single microtubule exhibited an obvious absence of fluorescence at a point previously fluorescent as shown in Fig. 1. The total number of cells observed and the duration of observation is summarized in Table 1. Relative breaking rates were estimated at defined curvatures by fitting a line to the cumulative distributions in the neighborhood of a specific curvature. Window sizes for line fitting varied from 0.25 rad/μm at low curvatures up to 1.0 rad/μm at high curvatures. The ratio of the slopes was then used to estimate the relative breaking rate.

Table 1. Summary of microtubule breaking observations

Cell	Number of breaks	Total microtubule length (μm)	Total time (minutes)	Breaking rate (breaks•mm^{-1}•minute^{-1})
1	0	70.2	2.47	0.0
2	3	100.9	2.45	12.1
3	2	200.9	3.97	2.5
4	0	237.5	3.95	0.0
5	1	179.0	3.95	1.4
6	1	152.0	3.97	0.9
7	0	201.2	2.47	0.0
8	1	287.7	3.97	0.9
9	5	185.0	2.47	11.0
10	4	301.9	2.95	4.5
11	0	667.8	2.95	0.0
12	3	211.1	3.95	3.6
13	0	224.2	3.95	0.0
14	4	135.2	2.46	12.0
Total	24	3,155	45.91	2.3±0.5

Note: not all microtubules could be observed for the total duration of the sequence. To obtain the breaking rate, the length and time were multiplied for each microtubule and these products added to obtain the denominator for the breaking rate calculation. The standard deviation for the breaking rate was obtained by dividing the mean rate by the square root of the number of observations as expected for a Poisson process.

RESULTS AND DISCUSSION

Quantitative analysis of microtubule bending and breaking

Individual breaking events were observed as shown in Fig. 1 and the curvature measured along the length of individual microtubules at the leading edge of Swiss 3T3 fibroblasts. The breaking was unlikely a direct result of photodamage as the fluorescent illumination was brief (100 milliseconds), infrequent (3-10 seconds apart), and breaking did not appear to occur more frequently at the end of the ~3 minutes sequences than at the beginning. To determine whether curvature in turn influenced breaking, the curvature of microtubules was measured at the breaking point immediately prior to breaking. Curvature changed little from frame to frame

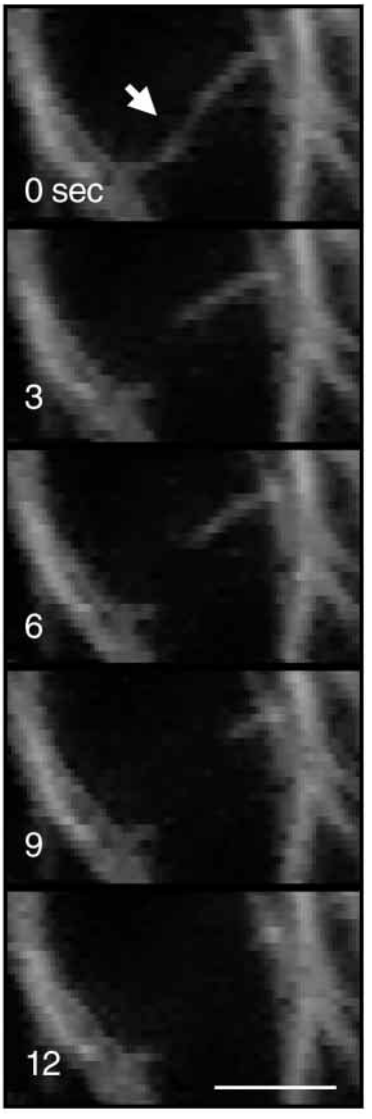

Fig. 1. Videomicroscopic observation of microtubule bending and breaking in living fibroblasts. A breaking event occurred between the 0 and 3 second time points in the vicinity of the white arrow. The newly exposed microtubule end in the upper right (designated as 'plus') disassembled, while the newly exposed end in the lower left (designated as 'minus') neither assembled nor disassembled ('paused'). Microtubules were often too close together to resolve as single microtubules and such microtubules were excluded from the analysis. Curvatures were measured as described in the Materials and Methods. Bar, 2 μm.

and when highly curved segments occurred they often persisted for several frames and were not necessarily broken immediately upon curving. Together these observations indicate that it is likely the curvature measured in the frame prior to the breaking event provided a good estimate of the curvature at the point where a microtubule broke. As shown in Fig. 2, the curvature of the microtubules that broke (mean = 1.5 rad/μm, sd = 1.0 rad/μm, n=24) was significantly larger than the curvature of the microtubule population as a whole (mean = 0.39 rad/μm, sd = 0.53 rad/μm, n=858, P<0.001). As others have asserted previously, microtubule curvature was likely the result of forces exerted by microtubule motors and/or actomyosin cortical flow (Vorobjev et al., 1997; Waterman-Storer and Salmon, 1997). Regardless of the specific curvature-inducing mechanism, the present results show that increasing curvature results in a greater likelihood of breaking.

In a previous report of mean microtubule curvature at breakage measured for a limited number of microtubules (n=7) in newt lung cells, the mean curvature was estimated to be 1.7 rad/μm (Waterman-Storer and Salmon, 1997). This previous value compares well with the present value (1.5 rad/μm) but is difficult to interpret further because the background curvature was not given in the previous report. Qualitatively, the present results are consistent with previous analyses indicating that breaking correlates with higher-than-normal curvature (Vorobjev et al., 1997; Waterman-Storer and Salmon, 1997). However, in these previous studies Waterman-Storer and Salmon commented that breaking occurred only on highly curved microtubules and Vorobjev et al. indicated an association between buckling/curving and breaking, whereas in the present study relatively straight microtubules were also observed to break on occasion. This difference may be due to fundamental differences between cell types since the previous results were obtained using epithelial cells and the present results were obtained using fibroblasts. That straight microtubules broke is not entirely surprising given that the ATP-dependent microtubule severing enzyme katanin can, at nanomolar concentrations, sever straight microtubules assembled in vitro from purified tubulin (Gross et al., 1998; McNally and Vale, 1993). Two other ATP-independent microtubule severing proteins, EF-1α and the homo-oligomeric protein p56, can also sever straight microtubules (Shiina et al., 1992, 1994).

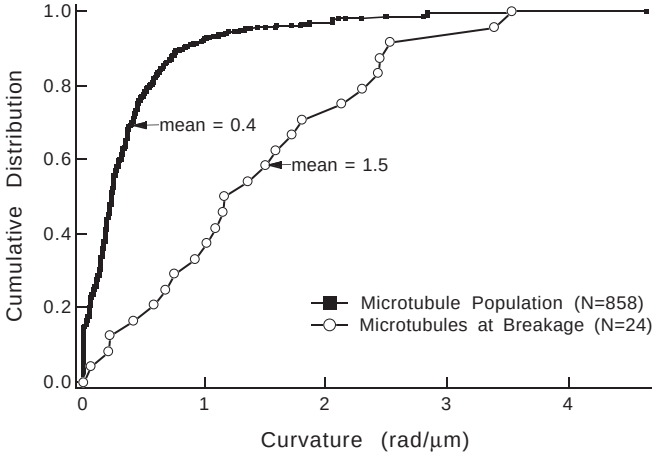

Fig. 2. Cumulative distributions of microtubule curvatures and the microtubule curvature at breakage. The mean for those that broke was significantly higher than the mean for the population as a whole (P<0.001).

Relationship between bending energetics and breaking kinetics

The forces that mediated the microtubule curving could not be estimated because the manner in which the forces were applied to the microtubules was not known. For example, different forces can give rise to the same local curvature depending on whether the microtubule can freely rotate about the point where force is applied (hinged boundary condition) or not (clamped boundary condition). More generally, it was not possible to determine whether stress, strain, or strain energy mediated the influence of deformation on the breaking rate since the three quantities are related. Converting curvatures to energies has the advantage that it facilitates straightforward relations between mechanics and chemical thermodynamics of microtubule processes such as breaking. Given an estimate of the flexural rigidity, EI, then curvature, dθ/ds, can be converted into free energy, F, by the relation (Landau and Lifshitz, 1970)

$$F = \tfrac{1}{2}EI\left(\frac{d\theta}{ds}\right)^2, \quad (1)$$

Assuming a flexural rigidity of 5.0×10^{-23} Nm^2, reported for tau- and MAP$_2$-coated microtubules in vitro (Tran et al., 1995), the mean curvature of 0.4 rad/μm for unbroken microtubules corresponded to an estimated mean free energy increase in the microtubule lattice of only ~0.5 kT/dimer. This energy is small compared to ~20 kT/dimer for the GTP hydrolysis associated with microtubule assembly, indicating that the potential of microtubules to do useful work in the cell by bending is minimal compared to the potential associated with assembly (assembly-associated movement reviewed by Inoué and Salmon, 1995). Note that this value for EI was in the middle of a range reported using laser tweezers at curvatures similar to those measured in the present study (cf. Felgner et al., 1996, 1997; Kurachi et al., 1995; Kurz and Williams Jr, 1995). The estimated mean energy increase was relatively small and within the range of normal energy fluctuations, ~1 kT/dimer (Hill, 1986). The mean curvature of microtubules that broke (1.5 rad/μm) corresponded to an energy of 8 kT/dimer, large enough to potentially influence the thermodynamics of microtubule-associated processes such as breaking. At the extreme, the most highly curved microtubules had energies up to ~40 kT/dimer.

The acceleration of breaking with increasing free energy of curving was estimated from the cumulative distributions in Fig. 2. Since the probability density is the first derivative of the cumulative distribution, estimating the slope of the cumulative distribution for microtubules that broke and dividing it by the slope of the cumulative distribution for microtubules that did not break provided a measure of the relative breaking rate as a function of curvature. Normalizing this relative breaking rate so that straight microtubules had a rate of unity and converting the curvatures into energies as described above (Eqn 1), it was found that the relative breaking rate increased ~40-fold as the energy increased to levels exceeding thermal fluctuations as shown in Fig. 3. Note that even a modest energy increase of ~2 kT/dimer led to a ~5-fold increase in the breaking rate.

If the acceleration of breaking were mediated simply by the

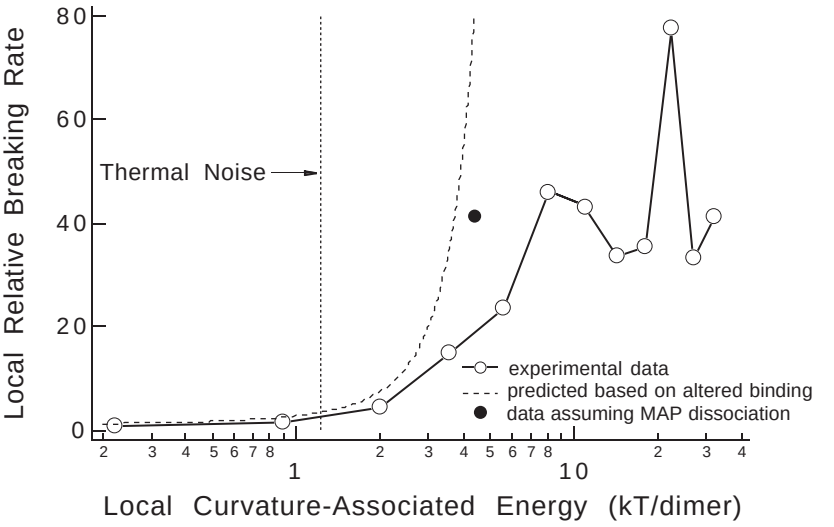

Fig. 3. Relationship between bending and breaking. The breaking rate increased ~40-fold as the energy associated with curvature increased above thermal noise levels, ~1 kT/dimer (open circles). If the energy associated with curvature directly influenced the thermodynamics of microtubule binding events that mediate breaking, then the increase should follow $e^{F/kT}$ (broken line). Deviations at the highest curvature may be accounted for if it is assumed that curving promotes MAP dissociation, which in turn lowers EI and the energy associated with curving. The highest curvature point is replotted at the lower energy corresponding to a microtubule where MAPs have dissociated (single black dot).

modulation of microtubule binding kinetics (and hence microtubule-binding thermodynamics) of a breakage-mediating protein, then an a priori prediction can be made regarding the expected degree of acceleration as a function of elastic energy increase. Specifically, a change in the relative on- and off-rates (k_{on} and k_{off}, respectively) given by an equilibrium constant, $K = k_{on}/k_{off} = e^{F/kT}$, will occur as a direct result of a change in free energy associated with curving (Hill, 1981). The broken line in Fig. 3 represents this theoretical relationship and provides reasonable agreement at low curvature, but not at high curvature. At high curvature the uncertainty in the breaking rate increases because of the relative infrequence of highly-curved microtubules. This uncertainty seems too small to account for the deviation from the theoretical prediction as the point estimates for the rate at high curvatures vary by ~40% while they deviate from the theoretical prediction by a factor of >1000.

Alternatively, it is possible that the value of flexural rigidity used to estimate the energy is not correct. From flexural rigidity studies in vitro it has been found that microtubule rigidity is generally lower for naked microtubules than for microtubules coated with MAPs, although there is considerable variability both in values for EI and the methods used to estimate EI. From the study by Tran et al. (1995) EI is ~6.9×10^{-24} Nm^2 for microtubules in the absence of MAPs (cf. Felgner et al., 1996, 1997; Kurz and Williams Jr, 1995; Venier et al., 1994). If curving caused MAPs to dissociate from microtubules, then EI would decrease with increasing curvature in vivo. Since it is not known what precise mathematical relationship exists between EI and curvature in vivo, it was tentatively assumed that at the highest curvatures EI dropped to naked microtubule levels and the energies recalculated. From Fig. 3 it can be seen that such an accounting of MAP dissociation lowers the estimated energy associated with curving and brings the data for the highest curvature into approximate agreement with the theoretical prediction. Thus, one interpretation of the results is that increasing curvature increases MAP dissociation, which in turn lowers the rigidity and makes the microtubule more accessible to severing enzymes, possibly the microtubule-severing ATPase katanin (McNally and Vale, 1993). Given the uncertainty in the appropriate value for flexural rigidity and uncertainty about the linearity of the elasticity, it is difficult to conclusively determine the reasons for the discrepancy between the data and the theoretical prediction.

Other possible mechanisms for the curvature-sensitivity include curvature-sensitivity of severing proteins and/or the tubulin dimers themselves. The latter possibility seems less likely as experiments in vitro with purified tubulin demonstrated the self-healing of lattice defects by free tubulin in solution, although the effect of curvature was not explicitly investigated and the microtubules generally had low curvature (Dye et al., 1992). In addition, buckling of naked microtubules in vitro (using laser tweezers) to the most extreme curvatures observed in the present study does not result in breaking, even when held highly curved for up to an hour (D. J. Odde and S. P. Gross, unpublished observations with taxol-stabilized microtubules; P. Tran, personal communication). Furthermore, it was found in the present study that in vivo even relatively straight microtubules can break occasionally, suggesting a severing process. As noted above, all three of the identified microtubule severing proteins (katanin, EF-1α, and p56) can sever straight microtubules. While the detailed mechanisms of the severing process are not known, Shiina et al. (1992) suggested that p56 acts to produce kinks or disorders in the microtubule since p56 localizes to kinks and breaks in microtubules. Alternatively, Waterman-Storer and Salmon (1997) suggested that severing proteins could bind preferentially to pre-existing defects in microtubules and promote further destruction of the microtubule lattice once bound. The present results do not permit discrimination between these two models. However, the breaking of straight microtubules in vivo coupled with the lack of intrinsic breaking of curved microtubules in vitro suggests that severing proteins mediate breaking in vivo and that tubulin, MAPs, and/or severing proteins (which can be considered a subset of MAPs) have intrinsic curvature sensitivity. The various mechanisms by which curvature could result in increased microtubule breakage are depicted in Fig. 4.

Microtubule breaking rate

The data also indicate that breaking is potentially a major mechanism by which noncentrosomal microtubules are generated in the cell as suggested by Vorobjev et al. (1997) and Waterman-Storer and Salmon (1997). By normalizing the number of

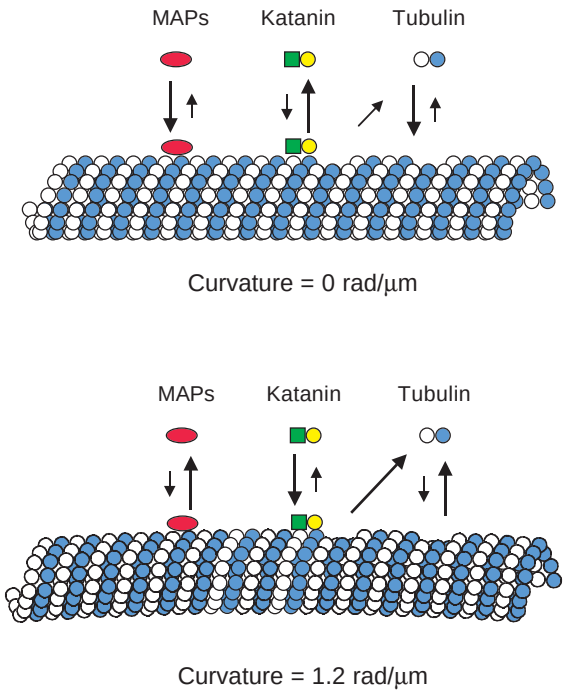

Fig. 4. Potential mechanisms for curvature-dependent microtubule breaking. Microtubule curvature could: (1) promote dissociation of MAPs which tend to stabilize microtubules, (2) promote binding and enzymatic activity of microtubule severing proteins such as katanin, and/or (3) promote dissociation of tubulin dimers directly from the lattice. The mechanisms are not mutually exclusive and are potentially synergistic. For example, dissociation of stabilizing MAPs could in turn promote association of katanin by increasing the number of sites available for katanin binding. The degree of curvature depicted (1.2 rad/μm) is drawn to scale and is approximately equal to the median curvature of microtubules that broke. While this curvature appears to be quite gentle, it corresponds to an energy of ~5 kT/dimer (assuming $EI=5\times10^{-23}$ Nm^2). The illustration is not meant to depict any particular mechanism of lattice deformation as there is currently no information available in this regard. Also, the depiction of the manner in which a severing protein binds to the lattice is speculative as well since it could bind to the ends or sides of tubulin dimers and could do so as an oligomeric complex instead of a single unit.

individual microtubule breaking events over the total microtubule length-time of observation, a specific breaking rate of 2.3 breaks·mm^{-1}·$minute^{-1}$ was estimated (sd = 0.5 breaks·mm^{-1}·$minute^{-1}$, n=24) as summarized in Table 1. The only other report in the literature of a specific breaking rate is 0.0016 breaks·$microtubule^{-1}$·$minute^{-1}$, corresponding to an upper limit of ~0.8 breaks·mm^{-1}·$minute^{-1}$ (if an average microtubule length of 20 μm is assumed) in epithelial cells (Vorobjev et al., 1997). For an interphase cell with 250 microtubules of 20 μm average length, our estimated specific breaking rate corresponded to ~11 breaks/minute over the entire cell, which is faster than the rate of centrosomal microtubule release in epithelial cells, ~1.5 released/minute for PtK1 cells (Keating et al., 1997) and ~0.02 released/minute for newt lung cells (Waterman-Storer and Salmon, 1997). Spontaneous nucleation was not observed in the present study as was previously reported for epithelial cells, which for a cell with 250 microtubules would give rise to ~3 new microtubules per minute based on the rate reported (Vorobjev et al., 1997). Although Vorobjev et al. concluded that nucleation was more frequent than breaking in epithelial cells, the present results lead to the opposite conclusion in Swiss 3T3 fibroblasts which suggests that system-to-system variability influences the relative contributions of breaking, nucleation, and centrosomal release to new microtubule generation in the cell. In any event, microtubule breaking is likely a major mechanism by which noncentrosomal microtubules are generated in some systems, consistent with the model proposed by Waterman-Storer and Salmon (1997, Fig. 12).

Fates of newly generated plus and minus microtubule ends

Consistent with earlier analysis of microtubule breaking in newt lung cells (Waterman-Storer and Salmon, 1997), newly exposed ends went into either a ‘pause’ state where neither assembly nor disassembly was apparent over the initial 3-10 seconds after breaking (11 plus ends, 13 minus ends) or went into a shortening state (9 plus ends, 7 minus ends; 4 plus ends and 4 minus ends could not be tracked unambiguously). Microtubules tending to point toward the leading edge were designated ‘plus’, while those tending to point away from the leading edge were designated ‘minus’. The observed shortening was unlikely a result of actomyosin-mediated retrograde flow, which was estimated to be <0.5 μm/minute, since shortening occurred at ~10 μm/minute. That some plus ends did not immediately disassemble was somewhat surprising since 100% of new plus ends generated by breaking in the study by Waterman-Storer and Salmon (1997, Table 3) were reported to go into a disassembly state. However, the number of observations in the previous study was limited (n=11) and the two breaking sequences shown (Waterman-Storer and Salmon, 1997, Fig. 8) seem to exhibit plus end pausing initially. Vorobjev et al. state that newly generated plus ends behaved similarly to pre-existing plus ends, which were generally dynamic but occasionally included pauses (Vorobjev et al., 1997, Fig. 4D). It seems that newly generated plus ends can occasionally pause, although there may be variations in behavior between cell types and further investigation is necessary to resolve this issue. The two previous studies and the present study all report both pausing and shortening for nascent minus ends. Taken together, we conclude that breaking tends to promote microtubule depolymerization.

Physiological significance

The curvature dependence of microtubule breaking could serve a number of cellular functions. Curvature sensitivity could facilitate the maintenance of cell polarity by promoting selective severing of highly curved microtubules that have lost their ‘normal’ (i.e. plus-end distal to the centrosome) microtubule orientation. It could also facilitate breakdown of curved microtubule assemblies during cell division. For example, budding yeast deletion mutants of the kinesin-related protein kip3 have impaired ability to break down their mitotic spindles during anaphase and so accumulate curved microtubules (Straight et al., 1998). One possible explanation for the anomalous accumulation of curved microtubules is that kip3 mediates curvature-sensitive breaking. In this scenario, kip3’s deletion (and the deletion of other molecules that participate in the curvature-sensitive breaking) would result in accumulation of curved microtubules.

In addition, the results suggest a microtubule-based mechanism for fluid shear stress response. Specifically, mechanical stress on the cell likely increases microtubule curving, which, according to the present results, will promote microtubule breaking and subsequent microtubule depolymerization. Microtubule depolymerization could then induce NF-κB-dependent genes (Rosette and Karin, 1995) which mediate the fluid shear stress response in vascular endothelial cells, including the increased expression of platelet-derived growth factor, PDGF (Khachigian et al., 1995). Through this chain of events, a mechanical insult (fluid shear stress) could induce the expression of a growth factor (PDGF) that promotes cell proliferation and wound healing.

This work was supported by the National Science Foundation.

REFERENCES

Buxbaum, R. E. and Heidemann, S. R. (1992). An absolute rate theory model for tension control of axonal elongation. *J. Theor. Biol.* **155**, 409-426.

Canman, J. C. and Bement, W. M. (1997). Microtubules suppress actomyosin-based cortical flow in *Xenopus* extracts. *J. Cell Sci.* **110**, 1907-1917.

Dye, R. B., Flicker, P. F., Lien, D. Y. and Williams Jr, R. C. (1992). End-stabilized microtubules observed in vitro: stability, subunit interchange, and breakage. *Cell Motil. Cytoskel.* **21**, 171-186.

Felgner, H., Frank, R. and Schliwa, M. (1996). Flexural rigidity of microtubules measured with the use of optical tweezers. *J. Cell Sci.* **109**, 509-516.

Felgner, H., Frank, R., Biernat, J., Mandelkow, E. M., Mandelkow, E., Ludin, B., Matus, A. and Schliwa, M. (1997). Domains of neuronal microtubule-associated proteins and flexural rigidity of microtubules. *J. Cell Biol.* **138**, 1067-1075.

Gittes, F., Mickey, B., Nettleton, J. and Howard, J. (1993). Flexural rigidity of microtubules and actin filaments measured from thermal fluctuations in shape. *J. Cell Biol.* **120**, 923-934.

Gross, S. P., McNally, F. J., Weitz, D., Block, S. M. and Odde, D. J. (1998). Dynamics of katanin-mediated microtubule severing in vitro. *Ann. Biomed. Eng.* **26**, S-72.

Hill, T. L. (1981). Microfilament or microtubule assembly or disassembly against a force. *Proc. Nat. Acad. Sci. USA* **78**, 5613-5617.

Hill, T. L. (1986). *An Introduction to Statistical Thermodynamics*. Mineola: Dover.

Inoué, S. and Salmon, E. D. (1995). Force generation by microtubule assembly/disassembly in mitosis and related movements. *Mol. Biol. Cell* **6**, 1619-1640.

Keating, T. J., Peloquin, J. G., Rodionov, V. I., Momcilovic, D. and Borisy, G. G. (1997). Microtubule release from the centrosome. *Proc. Nat. Acad. Sci. USA* **94**, 5078-5083.

Khachigian, L., Resnick, N., Gimbrone Jr, M. and Collins, T. (1995). Nuclear factor-kappa B interacts functionally with the platelet-derived growth factor B-chain shear-stress response element in vascular endothelial cells exposed to fluid shear stress. *J. Clin. Invest.* **96**, 1169-1175.

Kurachi, M., Hoshi, M. and Tashiro, H. (1995). Buckling of a single microtubule by optical trapping forces: direct measurement of microtubule rigidity. *Cell Motil. Cytoskel.* **30**, 221-228.

Kurz, J. C. and Williams Jr, R. C. (1995). Microtubule-associated proteins and the flexibility of microtubules. *Biochemistry* **34**, 13374-13380.

Landau, L. D. and Lifshitz, E. M. (1970). *Theory of Elasticity*. Oxford: Pergamon Press.

Letourneau, P. C., Shattuck, T. A. and Ressler, A. H. (1987). 'Pull' and 'push' in neurite elongation: observations on the effects of different concentrations of cytochalasin B and taxol. *Cell Motil. Cytoskel.* **8**, 193-209.

McNally, F. J. and Vale, R. D. (1993). Identification of katanin, an ATPase that severs and disassembles stable microtubules. *Cell* **75**, 419-429.

Putnam, A. J., Cunningham, J. J., Dennis, R. G., Linderman, J. J. and Mooney, D. J. (1998). Microtubule assembly is regulated by externally applied strain in cultured smooth muscle cells. *J. Cell Sci.* **111**, 3379-3387.

Rosette, C. and Karin, M. (1995). Cytoskeletal control of gene expression: depolymerization of microtubules activates NF-κB. *J. Cell Biol.* **128**, 1111-1119.

Sammak, P. J. and Borisy, G. G. (1988). Direct observation of microtubule dynamics in living cells. *Nature* **332**, 724-726.

Savage, C., Hamelin, M., Culotti, J. G., Coulson, A., Albertson, D. G. and Chalfie, M. (1989). mec-7 is a beta-tubulin gene required for the production of 15-protofilament microtubules in Caenorhabditis elegans. *Genes Dev.* **3**, 870-881.

Schulze, E. and Kirschner, M. (1988). New features of microtubule behaviour observed in vivo. *Nature* **334**, 356-359.

Shiina, N., Gotoh, Y. and Nishida, E. (1992). A novel homo-oligomeric protein responsible for an MPF-dependent microtubule-severing activity. *EMBO J.* **11**, 4723-4731.

Shiina, N., Gotoh, Y., Kubomura, N., Iwamatsu, A. and Nishida, E. (1994). Microtubule severing by elongation factor 1α. *Science* **266**, 282-285.

Straight, A. F., Sedat, J. W. and Murray, A. W. (1998). Time lapse microscopy reveals unique roles for kinesins during anaphase in budding yeast. *J. Cell Biol.* **143**, 687-694.

Tanaka, E., Ho, T. and Kirschner, M. W. (1995). The role of microtubule dynamics in growth cone motility and axonal growth. *J. Cell Biol.* **128**, 139-155.

Tran, P. T., Parsons, S. F., Sterba, R., Wang, Z., Sheetz, M. P. and Salmon, E. D. (1995). Direct measurement of microtubule flexural rigidity with the laser trap. *Mol. Biol. Cell* **6**, 260a.

Venier, P., Maggs, A. C., Carlier, M.-F. and Pantaloni, D. (1994). Analysis of microtubule rigidity using hydrodynamic flow and thermal fluctuations. *J. Biol. Chem.* **269**, 13353-13360.

Vigers, G. P. A., Coue, M. and McIntosh, J. R. (1988). Fluorescent microtubules break up under illumination. *J. Cell Biol.* **107**, 1011-1024.

Vorobjev, I. A., Svitkina, T. M. and Borisy, G. G. (1997). Cytoplasmic assembly of microtubules in cultured cells. *J. Cell Sci.* **110**, 2635-2645.

Waterman-Storer, C. M. and Salmon, E. D. (1997). Actomyosin-based retrograde flow of microtubules in the lamella of migrating epithelial cells influences microtubule dynamic instability and turnover and is associated with microtubule breakage and treadmilling. *J. Cell Biol.* **139**, 417-434.

Zheng, J., Buxbaum, R. E. and Heidemann, S. R. (1993). Investigation of microtubule assembly and organization accompanying tension-induced neurite initiation. *J. Cell Sci.* **104**, 1239-1250.